Supporting Information

Kinetics of a Criegee intermediate that would survive high humidity and may oxidize atmospheric SO_2

Hao-Li Huang[a], Wen Chao[a,b], and Jim Jr-Min Lin[a,b,1]

[a] Institute of Atomic and Molecular Sciences, Academia Sinica, Taipei 10617, Taiwan

[b] Department of Chemistry, National Taiwan University, Taipei 10617, Taiwan

[1] To whom correspondence may be addressed. Email: jimlin@gate.sinica.edu.tw

Supporting Figures S1-S15

Supporting Tables S1-S3

Synthesis procedure

UV absorption spectra of relevant species: Fig. S1-S2

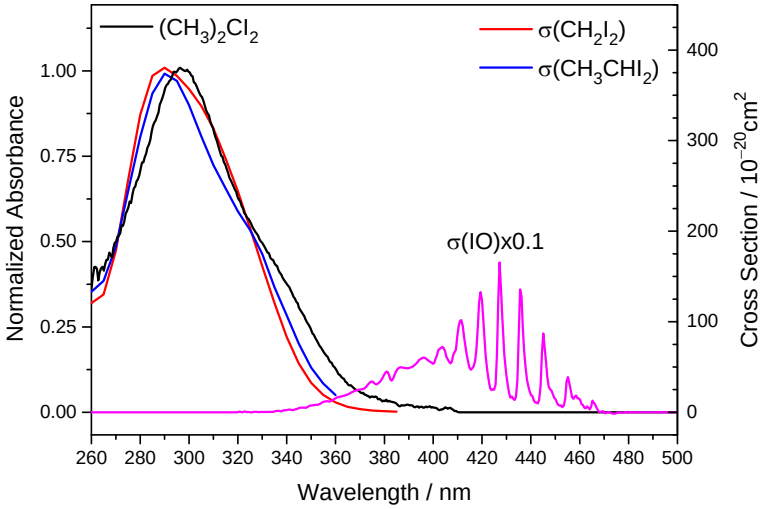

Fig. S1. UV absorption spectra of IO and C1 to C3 diiodoalkanes. The spectrum of $(CH_3)_2CI_2$ was measured by the iCCD spectrometer; the spectra of other species are from the literature (1). The maximum cross section of $(CH_3)_2CI_2$ was assumed to be the same as that of CH_2I_2, which is about $3.8x10^{-18}$ cm^2.

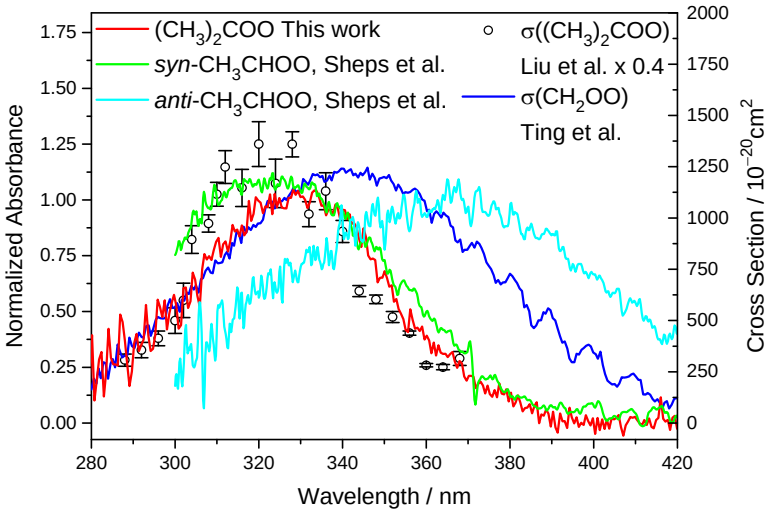

Fig. S2. Comparison of the UV spectra of $(CH_3)_2COO$ of this work and Liu et al. (2), CH_2OO (3), and *anti*- and *syn*-CH_3CHOO (4). The spectrum of $(CH_3)_2COO$ of this work is slight broader than the jet-cooled spectrum reported by Liu et al. (2). The contribution of hot bands in our room-temperature spectrum would cause broadening in comparison with the low-temperature spectrum of Liu et al. The absorption cross sections of CH_2OO and *syn*-CH_3CHOO are available (values shown as the right y-axis). For *anti*-CH_3CHOO and $(CH_3)_2COO$, their absolute cross section values have not been well determined yet; thus the peak-height normalized spectra are shown.

Experimental conditions of the $(CH_3)_2COO$ reactions with SO_2 and with H_2O: Tables S1-S2

Table S1. Summary for the experiments of the $(CH_3)_2COO$ reaction with SO_2. The absorption cross section of $(CH_3)_2CI_2$ (Me_2CI_2) was assumed to be about 3.8×10^{-18} cm^2 at 296 nm.

Exp #	*Laser fluence* / (mJ cm^{-2})	P_{Me2CI2} / mTorr	Maximum $\Delta Abs.$ (340 nm) $/10^{-3}$	P_{O2} / Torr	P_{Total} / Torr	k_0 fit / sec^{-1}	k_{SO2} / $10^{-11}cm^3sec^{-1}$	# of data points
1	3.4	1.19	0.879	11.0	20.1	423±90*	7.02±0.38*	6
2	10.0	2.26	7.71	10.5	49.9	1366±83	10.00±0.05	8
3	4.9	1.13	1.85	10.2	50.0	663±290	9.42±0.63	8
4	3.4	1.12	1.32	10.5	50.4	459±44	10.47±0.13	8
5	10.0	2.22	9.83	10.8	99.8	1749±127	11.55±0.07	8
6	10.0	2.27	10.5	10.4	100.0	1937±150	11.61±0.09	8
7	3.3	1.09	1.63	10.4	100.0	628±95	12.03±0.32	8
8	9.8	2.34	11.8	10.3	200.1	2077±246	12.17±0.15	8
9	9.9	2.26	11.5	10.1	300.0	1828±345	12.46±0.25	8
10	3.3	1.06	1.88	10.3	300.0	573±76	12.64±0.19	8
11	10.0	2.20	11.3	14.5	499.9	3206±401	12.83±0.16	8
12	3.5	1.19	2.83	21.6	770.4	1626±511	12.63±0.24	8
13	3.8	1.24	1.44	10.2	50.0 (Ne)	893±398	7.07±0.44	8
14	5.1	0.982	1.71	10.2	50.0 (CO_2)	990±191	11.38±0.49	8
15	8.6	1.60	5.70	10.5	10.5	1354±269	5.70±0.71	6
16	8.8	2.06	6.64	10.3	20.1	1328±96	8.70±0.28	8
17	5.3	1.32	2.82	10.3	20.0	763±219	7.67±0.88	6
18	5.2	1.22	2.77	10.0	35.0	560±334	9.36±0.87	8

* best fit value ± standard deviation.

Table S2. Summary for the experiments of the $(CH_3)_2COO$ reaction with H_2O. The cross section of $(CH_3)_2CI_2$ was assumed to be about 3.8×10^{-18} cm^2 at 296 nm. There was no obvious non-zero k_{H2O} observed; the detection limit for k_{H2O} was estimated to be $<1.5\times10^{-16}$ cm^3s^{-1}.

Exp #	*Laser fluence* / (mJ cm^{-2})	P_{Me2CI2} / mTorr	Maximum $\Delta Abs.$ (340 nm) $/10^{-3}$	P_{O2} / Torr	P_{Total} / Torr	k_0 / s^{-1}	k_{H2O}[§] / 10^{-17} cm^3s^{-1}	k_{w2}[§] / $10^{-14}cm^3s^{-1}$	# of data points
W1	4.3	3.02	5.49	20.2	200.2	1355	-1.8±3.8*	-0.52±2.9*	30
W2	5.1	0.97	1.65	21.8	200.1	654	2.9±1.7	2.5±1.2	27
W3	5.0	0.49	0.988	10.6	200.2	512	-0.56±2.8	-1.2±1.9	42
W4	2.2	0.48	0.448	10.5	200.1	483	4.9±4.0	3.7±2.8	21
W5	2.9	0.17	0.339	10.4	200.0	438	-0.048±2.4	-0.46±1.6	35
W6	3.2	2.58	3.1	21.7	200.0	895	10±3.7	7.7±2.6	13
W7	3.2	1.03	0.54	10.7	400.1	667	10±2.8	2.9±3.8	27
W8	3.4	1.17	1.33	10.8	500.0	697	3.7±4.9	6.7±2.1	28

* best fit value ± standard deviation.

[§] k_{H2O} and k_{w2} are the bimolecular rate coefficients of the $(CH_3)_2COO$ reactions with H_2O and $(H_2O)_2$, respectively. k_{H2O} is determined by assuming k_{w2} is zero; k_{w2} is determined by assuming k_{H2O} is zero.

Raw data and fit for Exp #1-18 of the SO_2 reactions with $(CH_3)_2COO$: Fig. S3-S9

Representative temporal profiles are plotted in Fig. S3-S6. All 138 pseudo-first-order rate coefficients are plotted in Fig. S7-S9 and Fig. 4 of the main text.

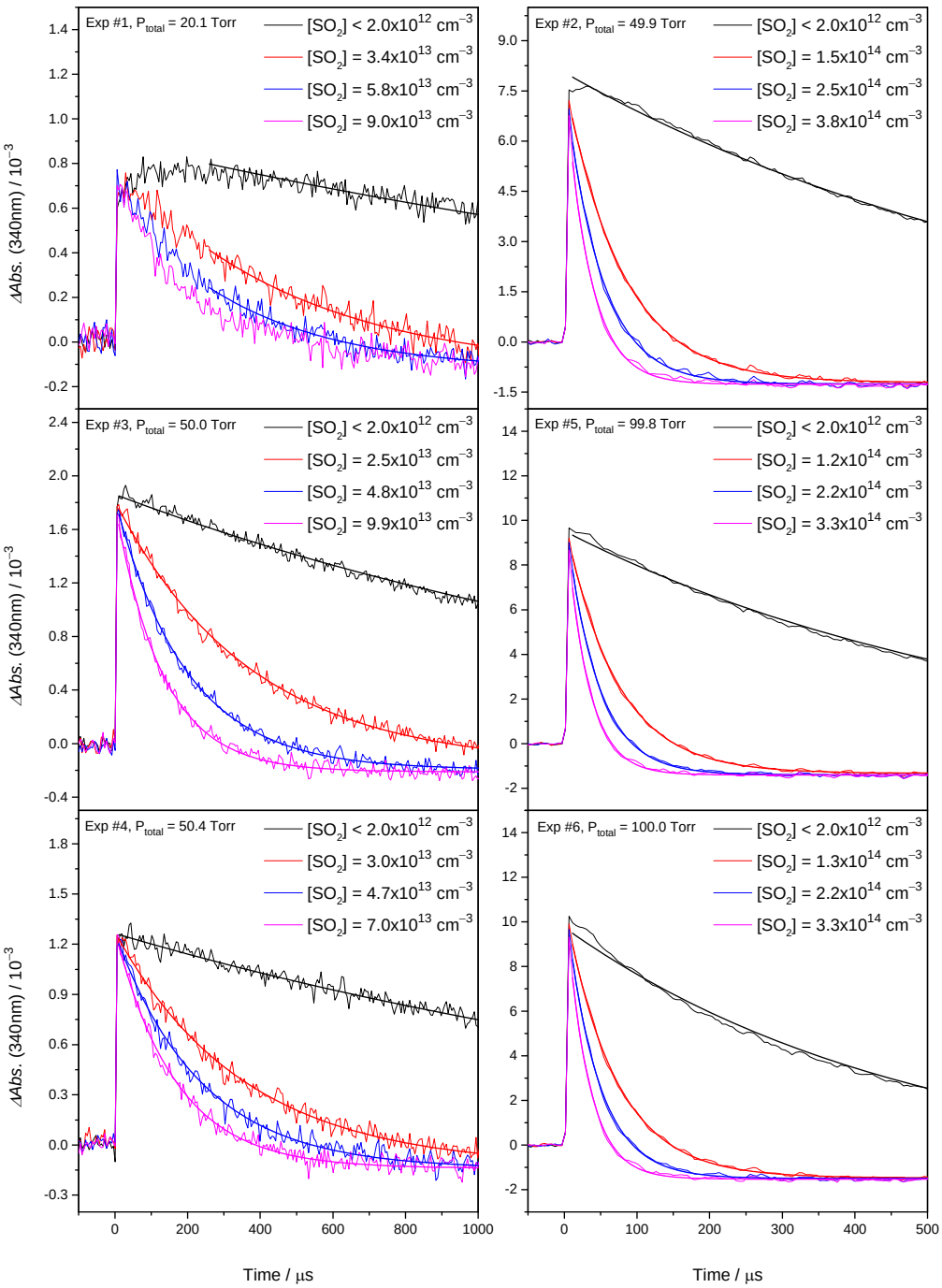

Fig. S3. Representative temporal profiles of the absorbance change under different $[SO_2]$ for Exp #1-6. The smooth lines are single exponential fit to the experimental data.

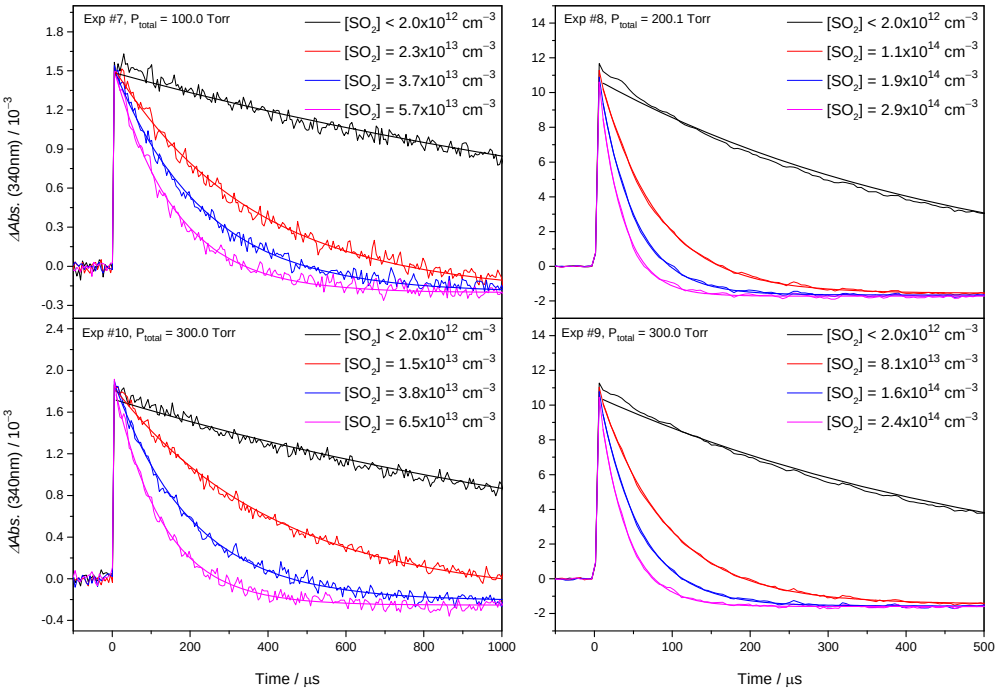

Fig. S4. Representative temporal profiles of the absorbance change under different [SO_2] for Exp #7-10. The smooth lines are single exponential fit to the experimental data.

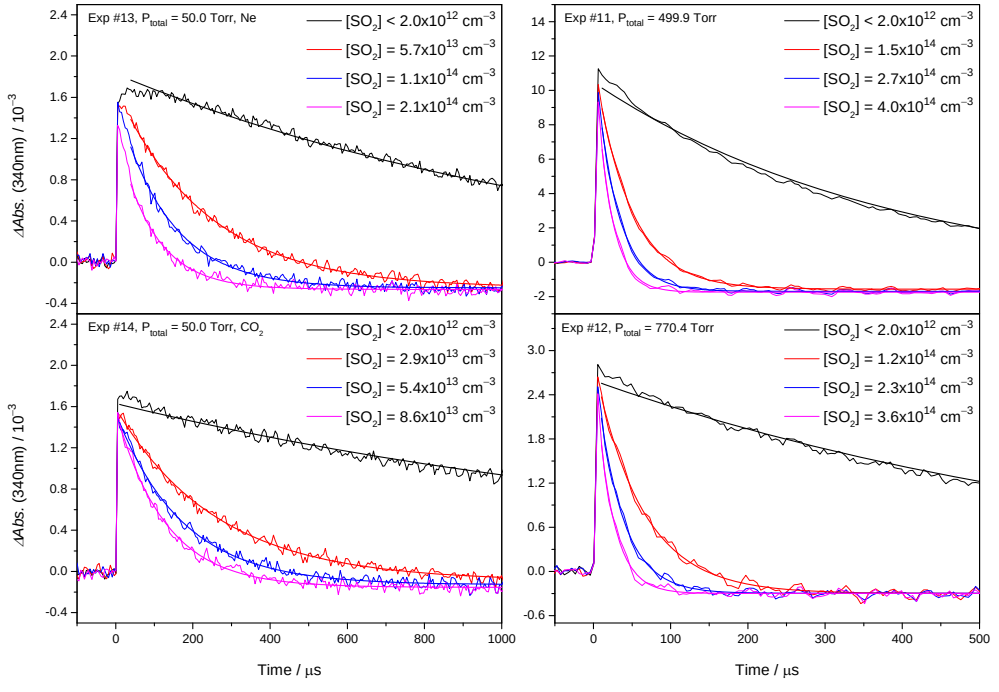

Fig. S5. Representative temporal profiles of the absorbance change under different [SO_2] for Exp #11-14. The smooth lines are single exponential fit to the experimental data.

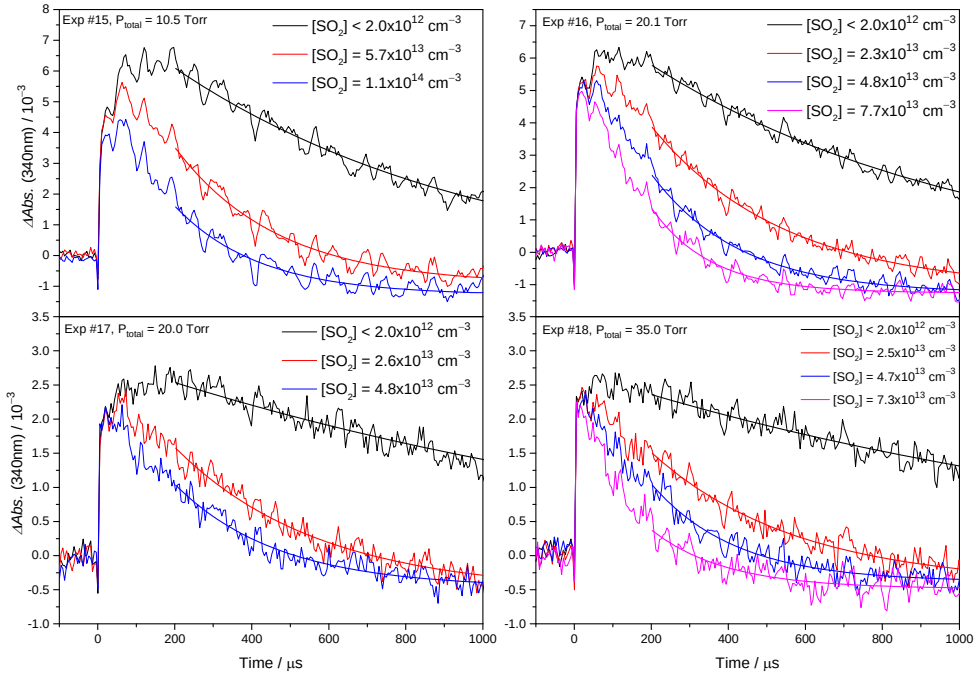

Fig. S6. Representative temporal profiles of the absorbance change under different $[SO_2]$ for Exp #15-18. The smooth lines are single exponential fit to the experimental data.

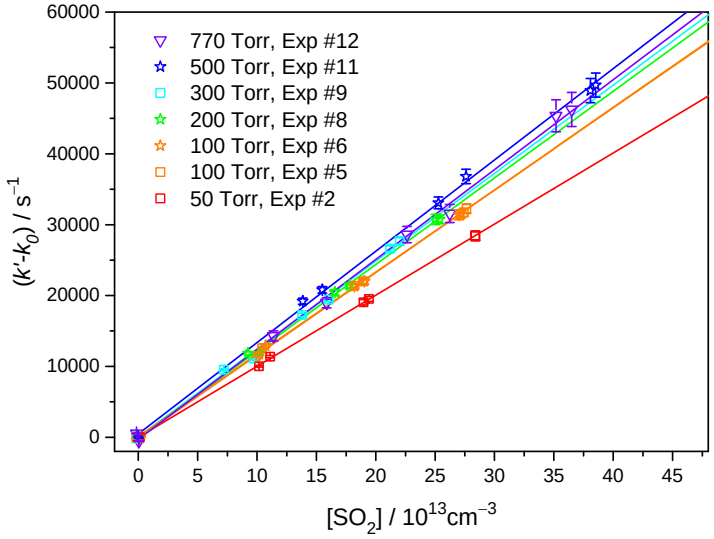

Fig. S7. Pseudo-first-order rate coefficient of $(CH_3)_2COO$ reaction with SO_2 plotted as a function of $[SO_2]$ at pressures of 50 to 770 Torr. k_0 is the rate coefficient at zero $[SO_2]$. The measurements were performed at 298 K with N_2 as the buffer gas at the indicated total pressure. Solid lines are linear fit at the corresponding pressure.

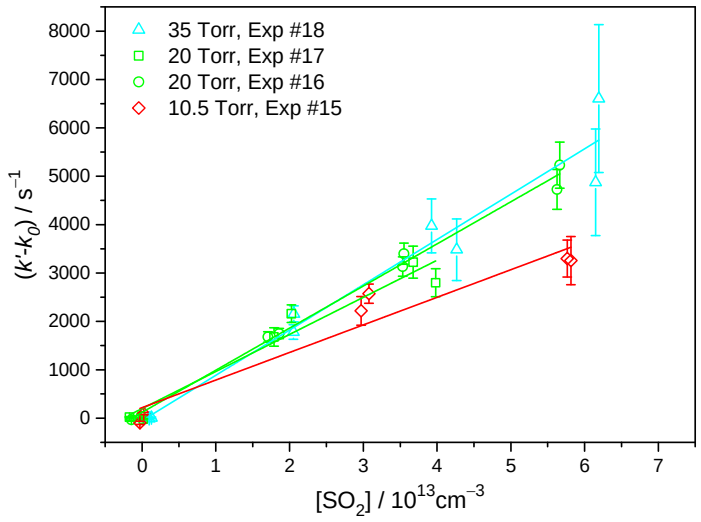

Fig. S8. Pseudo-first-order rate coefficient of $(CH_3)_2COO$ reaction with SO_2 plotted as a function of $[SO_2]$ at pressures of 10 to 35 Torr. k_0 is the rate coefficient at zero $[SO_2]$. The measurements were performed at 298 K with N_2 as the buffer gas to balance the total pressure, the partial pressure of O_2 is 10 Torr in each experiment set. Solid lines are linear fit at the corresponding pressure.

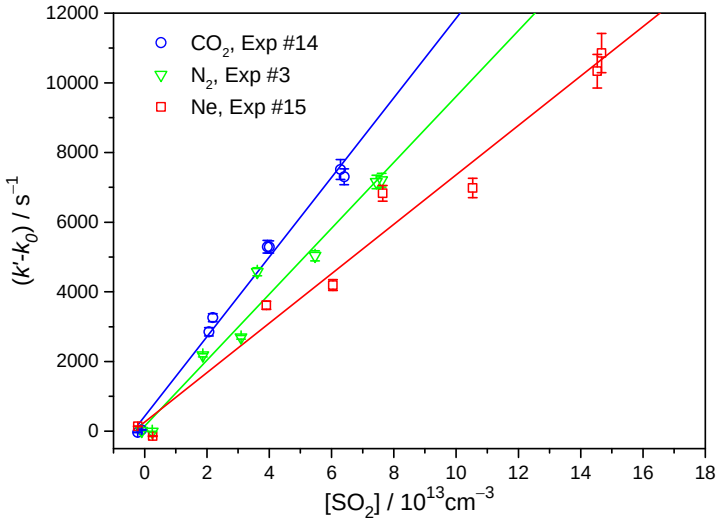

Fig. S9. Effect of the buffer gas in the reaction of $(CH_3)_2COO$ with SO_2. Pseudo-first-order rate coefficient of $(CH_3)_2COO$ reaction with SO_2 is plotted as a function of $[SO_2]$ for three buffer gases. k_0 is the rate coefficient at zero $[SO_2]$. The temperature was 298 K and the total pressure was 50 Torr with the indicated buffer gas (P_{O2} = 10.2 Torr). The data are fitted to a function of $k' - k_0 = k_{SO2}[SO_2]$. See Table S1 for the values of the rate coefficients.

Raw data and fit for Exp #W1-W8 of the H_2O reactions with $(CH_3)_2COO$: Fig. S10-S12

Representative temporal profiles are plotted in Fig. S10-S11. All 223 pseudo-first-order rate coefficients are plotted in Fig. 7 in the main text.

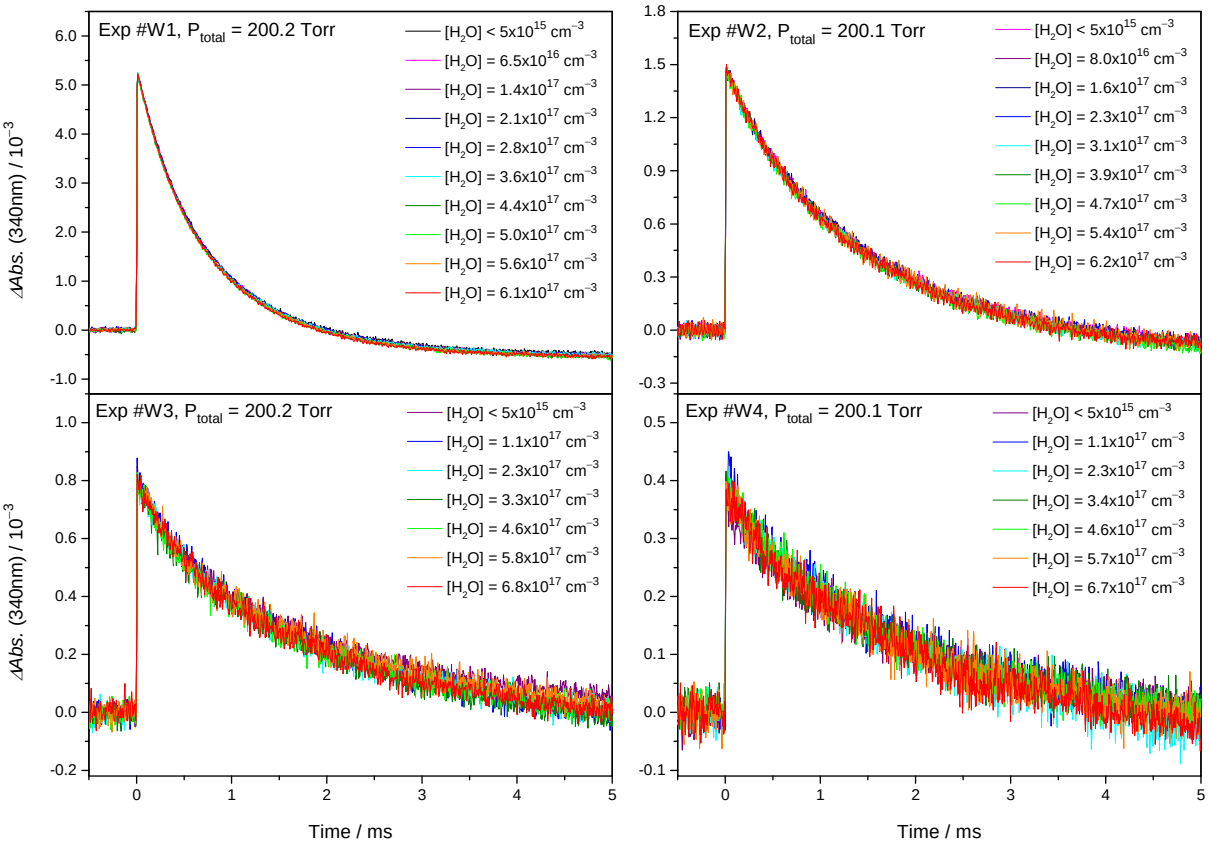

Fig. S10. Representative temporal profiles of the absorbance change under different $[H_2O]$ for Exp #W1-W4.

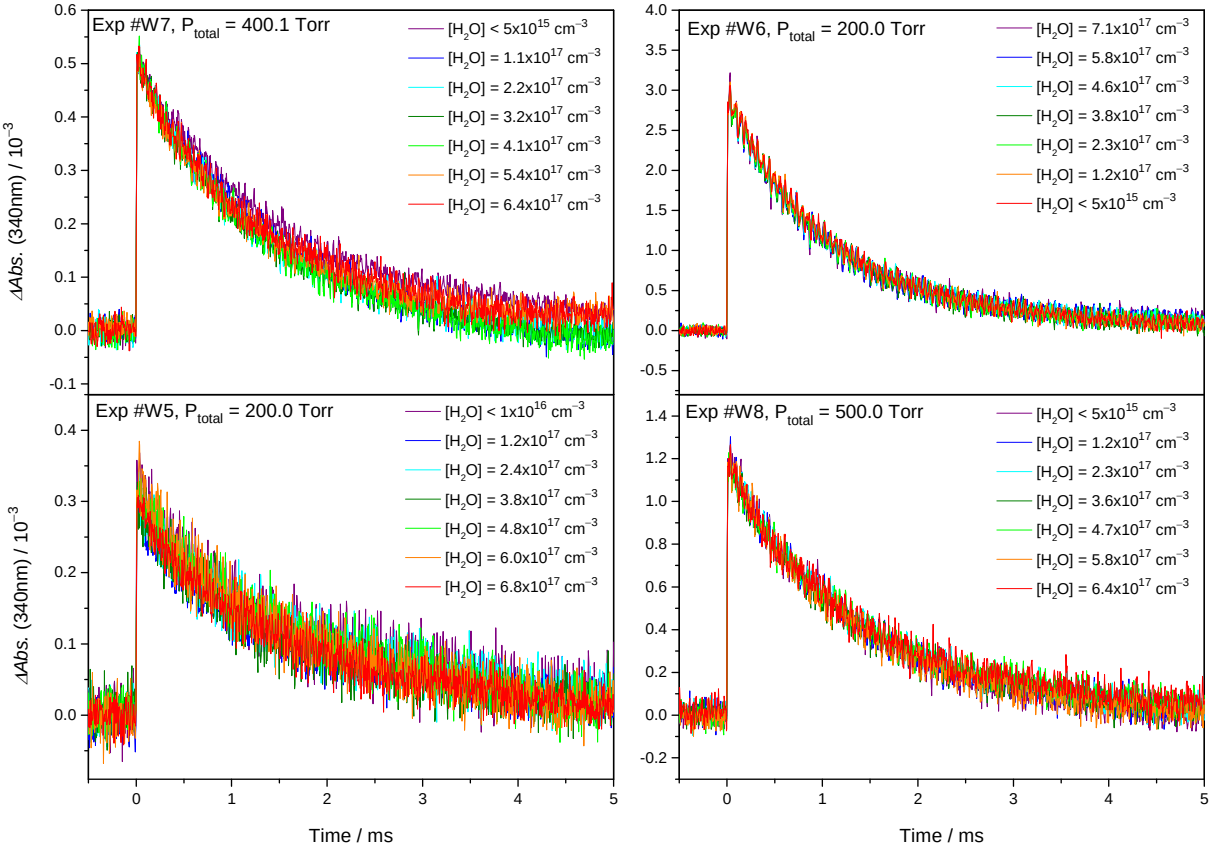

Fig. S11. Representative temporal profiles of the absorbance change under different [H_2O] for Exp #W5-W8.

$(CH_3)_2COO$ decay rate coefficient without adding the co-reactants (k_0)

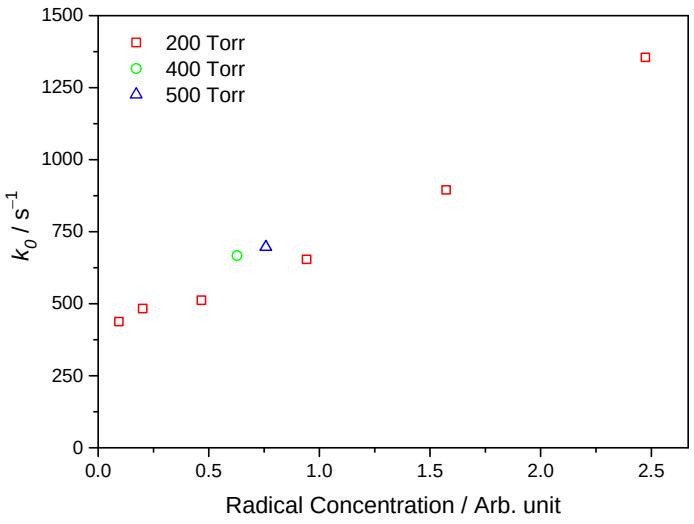

Fig. S12. Dependence of the $(CH_3)_2COO$ decay rate coefficient without adding the co-reactants (k_0 defined in the main text) on the total radical concentration, which is proportional to the product of the precursor concentration and the laser fluence. The maximum radical concentration in this Figure is estimated to be about $2x10^{12}$ cm^{-3}. Data are from Exp #W1-W8.

Data and analysis for the CH_2OO reaction with SO_2: Fig. S13-S15, Table S3

The pressure dependence on the rate coefficient of the CH_2OO reaction with SO_2 was investigated in this lab in order to have a more direct comparison with that of the $(CH_3)_2COO$ reaction with SO_2. The data and fit are shown below. A brief conclusion is that the pressure dependence (Fig. S15) is not obvious in the $CH_2OO + SO_2$ system.

Table S3. Summary for the experiments of the CH_2OO reaction with SO_2. The buffer gas is N_2.

Laser fluence / (mJ cm^{-2})	P_{CH2I2} / mTorr	Maximum $\Delta Abs.$ (340 nm) $/10^{-3}$	P_{O2} / Torr	P_{Total} / Torr	k_0 fit / sec^{-1}	$k_{CH2OO+SO2}$ / $10^{-11}cm^3sec^{-1}$	# of data points
13.6	1.03	2.96	9.66	30.1	298±70*	3.52±0.11*	10
13.8	0.92	2.68	9.7	51.1	148±26	3.46±0.04	9
13.9	1.03	2.48	9.78	99.7	66±57	3.72±0.07	10
7.13	2.28	10.1	9.92	100.1	408±58	3.69±0.03	8
5.04	1.15	3.08	9.96	100.2	174±17	3.57±0.02	9
13.9	1.17	2.12	9.82	199.7	90±78	3.70±0.10	10
5.18	1.28	1.82	9.75	350.3	287±125	3.59±0.17	9
4.4	1.67	1.31	9.61	755.6	0±272	3.30±0.33	8

* best fit value ± standard deviation.

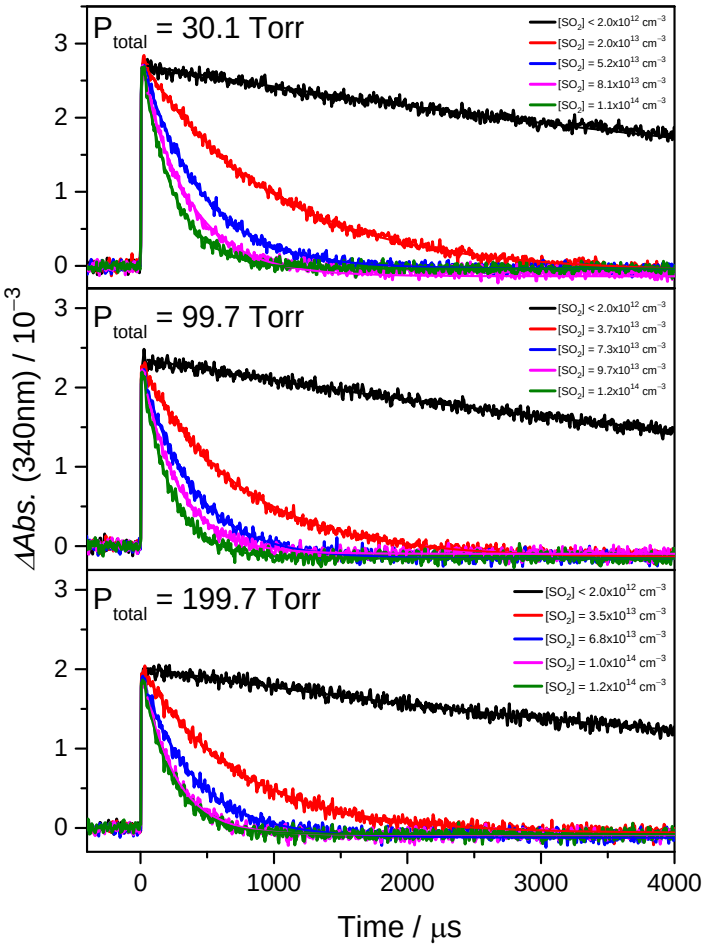

Fig. S13. Representative temporal profiles of the absorbance change of CH_2OO under different [SO_2] at selected total pressures. The buffer gas is N_2. The smooth lines are single exponential fit to the experimental data. See Table S3 for the experimental conditions.

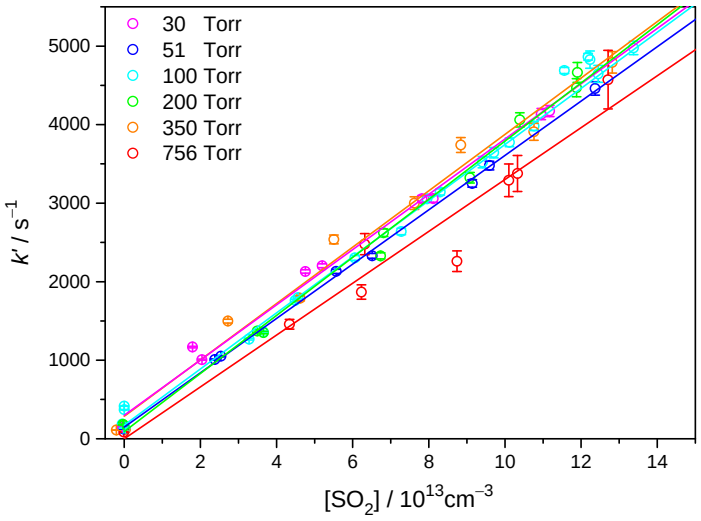

Fig. S14. Pseudo-first-order rate coefficient of CH_2OO reaction with SO_2 plotted as a function of [SO_2]. The measurements were performed at 298 K with N_2 as the buffer gas at the indicated total pressure. The error bars indicate the standard deviations; the number of independent data can be found in Table S3 for each experiment. Solid lines are linear fit to the data at the corresponding pressure.

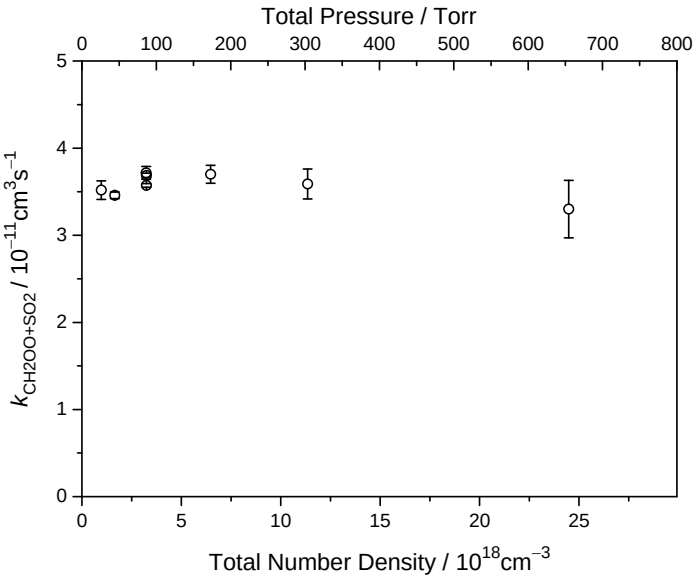

Fig. S15. Observed second-order rate coefficient of CH_2OO reaction with SO_2 plotted as a function of the total pressure. The error bars of the data indicate the standard deviations. There are total 8 independent measurements. See Table S3 for the experimental conditions.

Synthesis Procedure

The synthesis procedure of $(CH_3)_2CI_2$ is the following. Acetone (TEDIA, 99.98%) was added slowly to hydrazine monohydrate (Wako, 97%) with a dropping funnel while stirring vigorously. A boiling water bath was used for controlling the reaction temperature and the reaction time was at least 1 hour under reflux. Acetone hydrazone was extracted with CH_2Cl_2 (ACROS, 99.9%).

Saturated solution of iodine in ethyl ether (ALPS, 99.5%) was added at room temperature into a mixture consisting of acetone hydrazone, ether and triethylamine (Alfa Aesar, 99%) under dark condition. The reaction can be monitored by the evolution of nitrogen gas and persistence of iodine color. After the completion, the solution is diluted 20 times by adding ethyl ether. Then 5% $Na_2S_2O_{3(aq)}$ and 3M $HCl_{(aq)}$ are subsequently added to quench iodine and triethylamine. $(CH_3)_2CI_2$ is obtained by further washing the organic-phase solution with saturated $NaCl_{(aq)}$, drying and removal of solvent.

The structure and purity were checked with H-NMR spectroscopy (3.00 ppm (6H, s, Me) in $CDCl_3$). Minor amounts of acetone and 2-iodopropene were also found on the NMR spectrum. We estimated the purity of $(CH_3)_2CI_2$ was better than 85%. During the usage of $(CH_3)_2CI_2$, its purity became higher with time, possibly because the impurities have lower boiling points. The observed kinetic results of the Criegee intermediate do not depend on the purity of the $(CH_3)_2CI_2$ precursor in this study.

Supporting References

1. Sander SP, *et al.* Chemical Kinetics and Photochemical Data for Use in Atmospheric Studies, Evaluation Number 17, JPL Publication 10-6, Jet Propulsion Laboratory, Pasadena, 2011. http://jpldataeval.jpl.nasa.gov
2. Liu F, Beames JM, Green AM, & Lester MI (2014) UV Spectroscopic Characterization of Dimethyl- and Ethyl-Substituted Carbonyl Oxides. J Phys Chem A 118(12):2298-2306.
3. Ting W-L, Chen Y-H, Chao W, & Smith MC (2014) The UV absorption spectrum of the simplest Criegee intermediate CH_2OO. Phys Chem Chem Phys 16(22):10438-10443.
4. Sheps L, Scully AM, & Au K (2014) UV absorption probing of the conformer-dependent reactivity of a Criegee intermediate CH_3CHOO. Phys Chem Chem Phys 16(48):26701-26706.